Optical and Quantum Electronics (2024) 56:1825
https://doi.org/10.1007/s11082-024-07736-2

Optical beam steering in laser terminals for enhanced laser communication through component interaction evaluation

Micah Baleya[1] · Hossam Shalaby[2] · Kazutoshi Kato[3] · Maha Elsabrouty[1]

Received: 11 May 2024 / Accepted: 8 October 2024 / Published online: 4 November 2024

Abstract
Optical beam steering is essential for maintaining line-of-sight (LOS) connections between communicating terminals, ensuring reliable Free Space Optical (FSO) communication. However, achieving a LOS connection is challenging due to disturbances such as vibrations from communication terminal and/or the host of the terminal, which can misalign the optical beam. The accuracy of the optical beam position sensor, the controller for the beam actuation unit, and the actuation units impact the beam steering system's performance. While extensive research has emphasized the importance of fast-steering mirrors (FSMs) as actuators and quadrant detectors (QDs) as optical beam position sensors in beam steering systems, most of these studies have focused on analyzing FSMs and QDs in isolation. This paper proposes a method to design and evaluate the impact of these components concurrently. Specifically, it suggests a tuning procedure for the controller in the FSM closed feedback loop and models the QD sensor using experimental data. The QD model is then integrated into the FSM control loop. To validate the viability of this integrated approach, its results are compared to those obtained with an ideal sensor. Integrating the QD model into the FSM control loop slightly increases overshoot but a faster and more responsive control is attainable.

Keywords Free space optical (FSO) communication · Proportional integral derivative (PID) · Fast steering mirror (FSM) · Quadrant detector (QD) · Genetic algorithm (GA)

✉ Micah Baleya
micah.baleya@ejust.edu.eg

[1] Department of Electronics and Communications Engineering, Egypt Japan University of Science and Technology, New Borg El-Arab City, Alexandria 21934, Egypt

[2] Electrical Engineering Department, Faculty of Engineering, Alexandria University, Alexandria 21544, Egypt

[3] Graduate School of Information Science and Electrical Engineering, Kyushu University, Fukuoka-shi, Fukuoka 819-0395, Japan

1 Introduction

Free Space Optical (FSO) communication has gained popularity for its potential to overcome challenges encountered in radio frequency (RF) communication. It provides higher data rates, utilizes narrow and secure communication channels, and the transceivers require less power as compared to their traditional RF counterpart (Chaudhry and Yanikomeroglu 2020; Al-Gailani et al. 2020). To harness the advantages of FSO communication, establishing a line-of-sight (LOS) link between communicating terminals is essential. However, achieving LOS in FSO communication is challenging due to disturbances such as vibrations from the communication terminal and/or the host of the terminal, which can push the optical beam's pointing vector off the desired direction. Additionally, noise from the optoelectronics in the transceiver and the background noise negatively impact the performance of the optical beam steering system. Moreover, optical beam steering system's performance relies on the optical beam position sensor's accuracy, the effectiveness of controller for the actuation units, and the effectiveness of actuation units themselves. This necessitates the need for a robust beam steering system that performs effectively despite the negative influences.

The beam steering system consists of various components, such as fast steering mirrors (FSMs), gimbal mechanisms, look-behind mirrors, detectors, hand-over mirrors, optical beam-splitters, control electronics and algorithms, optical isolators and polarizers. Lately, there has been a surge in research focused on designing controllers for the FSMs and improving Quadrant Detector's (QD's) accuracy in detecting laser spot position. This interest is driven by the pivotal role these components play which highly affect the performance of optical beam steering system. Therefore, we concentrates on these critical components in this work. The QD detects the position of the incoming laser beam. The position information is passed to the Proportional Integral Derivative (PID) controller, which then generates a control signal to steer the beam in the required direction. The FSM responds to the control signal by adjusting its actions to ensure that the beam of light maintains its desired direction. The arrangement of these parts in the considered system is shown in Fig. 1.

Typically, the beam steering system employs two independent closed feedback control loops to precisely tilt the FSM along both the x-axis and y-axis. While we primarily focus on the control mechanism for the x-axis, the closed feedback control loop for the y-axis

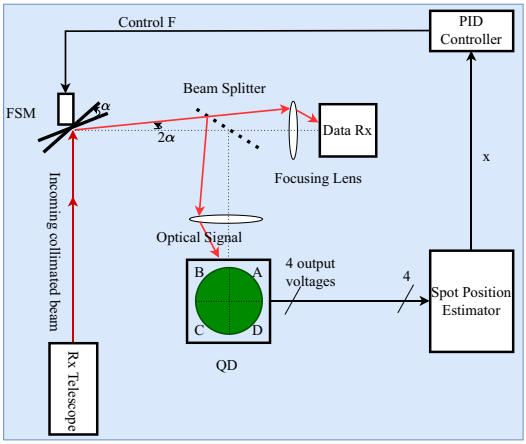

Fig. 1 An illustration of the system under consideration, depicting the closed feedback control loop of the FSM as it tilts along the x axis

operates similarly. This is how the system operates, collimated beam is reflected by the FSM onto the beam splitter. The splitter divides the beam into two parts: one part goes to the communication subsystem, and the other part is focused on the QD for position sensing. The QD then produces photoelectric currents, which are subsequently converted to voltages that act as feedback information for the control loop. In an ideal scenario, the control of the FSM relies on the precise laser position data provided by the QD. Depending on the incident light's position on the detector, the FSM is rotated accordingly.

1.1 Fast steering mirror control: state of the art and challenges

FSMs play a crucial role in optical beam steering systems. They offer high precision and rapid response, enabling fast and precise tracking. When installed in the optical path, FSMs control the direction of emitting and receiving optical axes to effectively addresses LOS challenges (Watkins et al. 2004; Zhou et al. 2009). However, achieving the LOS is challenging, because the terminal propagates the beam in free space which is plagued by the disturbances. The disturbances negatively affect the terminal, causing the pointing vector of the transmitted beam to misalign with the receiving end.

Chaudhary et al. presented a control loop design for FSM which is based on flexure hinges and specifically intended for precise beam pointing applications (Chaudhary et al. 2018). The authors compared two configurations, one with lead compensator and the other with a Ziegler Nicholas PID controller in the control loop. They evaluated and compared the models' performances on bandwidth and gain margin. The study contributes to the field by addressing modeling challenges and demonstrating the FSM's effectiveness in achieving high precision tracking and stabilization. Zhang et al. proposed an anti-disturbance strategy utilizing Adaptive Robust Control (ARC). They reported that their approach avoids amplifying the high-frequency noise, a common issue in traditional anti-disturbance methods like the disturbance observer. Furthermore, the use of an adaptive controller showed to decrease steady-state error (Zhang et al. 2019). Zhou et al. performed an investigation on the beam angle of the steering system, identifying critical factors that impact the design of FSM and the arrangement of the laser optics. The study highlighted the use of flexure hinges with compliant mechanisms in constructing the FSM structure and the application of a 4-QD as the the laser position sensor. The paper also discussed the control loop design that was developed and the fundamental concepts related to the FSM model (Zhou et al. 2009). Zhu et al. presented a system for steering optical beams that uses a dual-axis FSM equipped with piezoelectric actuators to achieve accurate pointing. The paper introduced a formulation of the FSM mathematical framework, that employs matrix transformation approach of a multibody system to describe dynamic characteristics and incorporating a model of hysteresis to depict the hysteresis. The mathematical framework serves as the basis for applying a hybrid control to accurately track the angle at which the FSM steers the laser beam (Zhu et al. 2015).

1.2 Machine learning techniques for improved beam position detection accuracy on quadrant detector

A QD has received significant attention from many scholars due to its crucial role in laser beam spot position detection and tracking (Zhang et al. 2015). It detects the incident laser beam and produces photoelectric signals corresponding to the position of beam spot on its surface. Nonetheless, the position of beam spot on the QD and the

Output Signal Offset (OSO) have a nonlinear relationship. There is high level of accuracy when detecting the beam spot position near the center of the QD. However, the further the spot moves from the center of QD, the less accurate the measurements become. Also, the unevenness of the QD's surface negatively affects position detection accuracy. It is important to note that the QD's detection accuracy influences the performance of subsequent modules within the transceiver.

To address the challenges related to QD detection, various strategies have been proposed by scholars. These strategies span from traditional methods such as curve fitting (Wang et al. 2020; Zhang et al. 2020; Silva and Van Vliet 2006), to approaches based on Artificial Neural Networks (ANNs). ANNs have demonstrated enhanced performance and more accurate models for QD laser spot position detection.

The study by Li et al. (2019), utilized the Levenberg-Marquardt (LM) algorithm and backpropagation learning, to develop an optimized Feedforward Neural Network (FFNN) model. This model performed better than eight-order polynomial fitting and the fusion approach. To overcome the challenge of gathering enough actual QD data for ANN training, Qiu et al. (2022) generated simulation QD data using mathematical formulas. A FFNN model was trained on this simulated data and on little amount of real data. This proposed approach surpassed the methods in Li et al. (2019) and the geometric approximation method detailed in Lu et al. (2014). In another study by Wang et al. (2021) proposed a technique for employing a Radial Basis Function Neural Network (RBFNN) model to determine the x and y coordinates of the light spot position on the QD. This model demonstrated superior performance compared to both the FFNN in Li et al. (2019) and seventh-order polynomial fitting. It was observed that single ANN solutions were used in all the earlier investigations. Individually, ANN models have inherent limitations. This results in their inability to properly learn all the complex underlying features and give a conclusive solution for generalizing a problem (Wu and Chen 2009). Our previous study (Baleya et al. 2023), proposed a neural network ensemble solution. The proposed solution showed that results on spot position predictions were more stable and detection accuracy improved. This was validated through superior performance of the ensemble model when compared to models in Li et al. (2019) and Wang et al. (2021), as well as to the RBNN and FFNN of the same complexity to that of the ensemble.

The contributions of our current work can be summarised as follows: we present a new closed-loop beam steering setup controlled using a genetic algorithm (GA)-tuned PID controller. In addition we consider a complete beam steering system simulation. While extensive scholarly research has highlighted the importance of both FSMs and QDs in beam steering systems, most of these studies have focused on analyzing FSMs and QDs in isolation. Recognizing that the functionalities of these components are interdependent, our study develops an integrated closed-loop beam steering system that considers both FSMs and QDs implemented together in a complete system. To assess the impact of the QD sensor on the entire system's performance, we have modeled the dynamics of the QD sensor using a FFNN and utilized the laser beam spot position estimation approach in Baleya et al. (2023). Furthermore, to validate the viability of the integrated approach, we have analyzed two scenarios: one with idealised sensor and the other with QD in the sensor path.

The remaining of the paper is arranged as follows: The next section discusses the compensation system for the FSM with an ideal sensor. After which, the simulation outcomes related to FSM control using an ideal sensor is presented. Next, the position sensing mechanism model is described. Following that, the integration of the QD model into the feedback control loop is explained. The section that follows, discusses the simulation results for

FSM control using a QD sensor. The final section summarizes the findings and implications of the study.

2 Proposed approach for modeling a compensation system for the FSM with an ideal sensor

The FSM is a device that is affixed actuators, enabling it to execute rapid and precise movements. Typically, these actuators are linear and are arranged in pairs per axis, allowing them to exert force on the mirror to induce tilts around the axis. The coordinate system for the mirror virtually originates at the mirror's center, and the actuators generate angular torque, resulting in minor rotations about the axes. Several actuator technologies are used to operate mirror movements: voice coil actuators, motorized actuators, piezoelectric (PZT) actuators and galvo motors.

Taking FSM as a standalone assembly, one can utilize a basic illustration that uses a spring and a damper system as an analogous setup. The elasticity of the flexure is essential in modeling the mirror since it is linked to the spring in the actual device, which generates oscillations. The damper, on the other hand, is dependent on air viscosity and guarantees smooth movement. The spring-mass-damper dynamical behavior is analogous to the classic second-order systems, and thus, its performance can be evaluated using second-order analysis methods. To this end, the transfer function for the FSM, adapted from Zhou et al. (2009), which is based on voice actuators, is given as follows:

$$G(s) = \frac{4.959 * 10^7}{s^2 + 130s + 102430} \tag{1}$$

The open loop performance of the FSM using transfer function (1) was examined in Zhou et al. (2009), which highlighted the need for a compensation mechanism for the FSM. This work therefore, focuses on designing the closed loop control for the FSM. The parameters considered during the design of the FSM control are displayed in Table 1, and are adapted from Chaudhary et al. (2018).

2.1 FSM closed loop control designing

This study, employs the PID controller for the compensation task. The choice of the PID controller stems from its ease of implementation and its effective performance when dealing with models that represent second-order linear differential equations. Initially, we aim to obtain a reasonably effective controller. This involves setting the initial controller parameters based on system knowledge and engineering intuition. The goal is to achieve stability, responsiveness, and acceptable performance. Leveraging information

Table 1 Design considerations (Chaudhary et al. 2018)

Parameter	Value
Close loop bandwidth	> 100 Hz
Step response overshoot	minimal or no overshoot
Step response rise time	1 m sec

about the initial controller parameters, an optimization algorithm is then applied. Through iterations, the controller parameters are fine tuned to enhance performance, minimize overshoot, and achieve desired system behavior.

The PID is a fixed gain controller with a closed loop control mechanism. In this control mechanism the error value $e(t)$ is constantly computed as the difference between the process variable $y(t)$ that is sensed and a desired set-point $r(t)$. The error's proportional, integral, and derivative values are calculated and then summed up to produce the control signal $u(t)$ that drives the plant (FSM). Figure 2 shows a typical PID controller.

The following mathematical expression defines the PID controller:

$$u(t) = K_p e(t) + K_i \int_0^t e(t)\,dt + K_d \frac{d}{dt} e(t). \tag{2}$$

Taking the Laplace transform and relating the output to the input of the controller yields the following generic transfer function:

$$G_c(s) = K_p + \frac{K_i}{s} + \frac{K_d \cdot s}{1 + \tau \cdot s}, \tag{3}$$

where, $G_c(s)$ is the controller's transfer function, K_p is the proportional gain, K_i is the integral gain, K_d is the derivative gain, τ is the time constant for the derivative filter and s is the complex frequency. In obtaining the initial controller parameters, Matlab SISO tool from the control system toolbox was used. This resulted in the following controller parameters; $K_p = 1.391 \times 10^{-3}$, $K_i = 2.189$, $K_d = 2.046 \times 10^{-5}$ and $\tau = 5.682 \times 10^{-4}$. These parameters yielded the following controller transfer function:

$$G_c(s) = \frac{0.0374s^2 + 4.637s + 3852}{s^2 + 1760 \cdot s}. \tag{4}$$

Using this controller on the FSM dynamics results in the response shown in Fig. 3 when a step reference signal is applied.

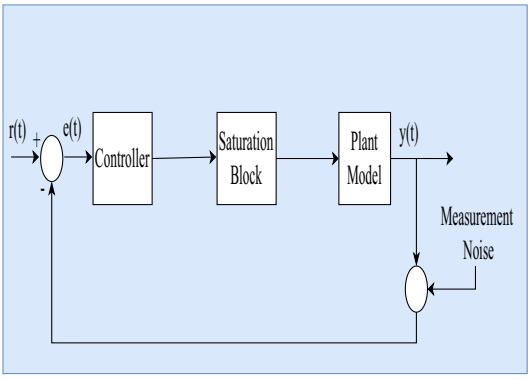

Fig. 2 A Proportional-Integral-Derivative (PID) controller

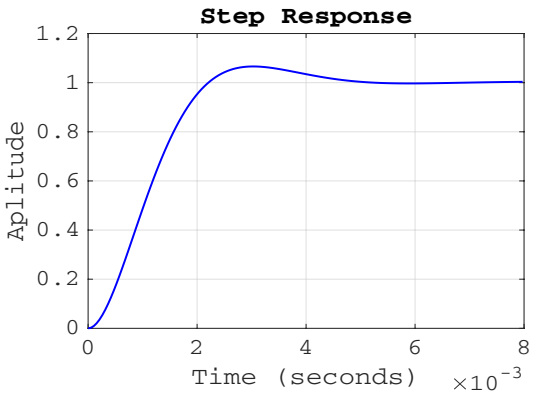

Fig. 3 Shows the response of the FSM with a controller tuned using the SISO matlab tool

2.2 Optimizing controller parameters with genetic algorithm

Natural selection and genetic principles serve as the foundation for the GA search and optimization method. It is a powerful technique that generates quality solutions to difficult optimization and search problems by utilizing biologically inspired operators including crossover, selection and mutation (Man et al. 1996). In each iteration, the algorithm chooses individuals from the existing population to serve as progenitors for the next generation. This method allows the population in subsequent generations to progressively evolve towards the optimal solution.

In this work, GA is used to find optimal controller parameters i.e K_p, K_i, K_d and τ. This is done by creating an initial population of possible solutions for the controller parameters and evolving the population until the optimal solution is found according to the specified cost function. Each of these solutions is represented by a string of symbols, and then by applying biological operators that is selection, crossover and mutation, new and better controller parameters are generated. Algorithm 1 shows the flow of our proposed GA based PID controller fine tuning.

Algorithm 1 Genetic Algorithm

$i \leftarrow 0$
Initialize population $P(i)$ based on SISO designed controller parameters
Input: $P(i)$, N (Number of generations)
Output: Optimal controller parameters
while $i \leq N$ **do**
    $i \leftarrow i + 1$
    $P_s(i) \leftarrow \text{Select}(P(i-1))$
    $P_c(i) \leftarrow \text{Crossover}(P_s(i))$
    $P_m(i) \leftarrow \text{Mutate}(P_c(i))$
    Evaluate the fitness of individuals in $P_m(i)$ using J
end while

In the suggested approach, the initial population is generated based on the knowledge of previously tuned controller using the SISO tool, this is to assist the algorithm narrow down the search space and enhance convergence. In assessing the goodness of the controllers, several error based fitness functions have been used in literature. These include, Integral Square Error (ISE), Integral Absolute Error (IAE), Integral Time Square Error (ITSE), Integral Time Absolute Error (ITAE), and Integral Square Time Error (ISTE) (Deniz et al. 2017; Jayachitra and Vinodha 2015). We utilized a fitness function proposed in Gaing (2004), which has been chosen based on the fact that it considers most of the time response performance parameters that are considered during controller designing such as overshoot (M_p), rise time (t_r), settling time (t_s) and steady state error (E_{ss}). It is defined as follows:

$$J(K) = (1 - e^{-\beta})(M_p - E_{ss}) + e^{-\beta}(t_s - t_r), \tag{5}$$

where K is a vector of controller parameters, and β is the weighting factor. The designer's requirements are met by utilizing the value of the weighting factor β. When β exceeds 0.7, it effectively reduces steady-state error and overshoot. Conversely, if the objective is to minimize settling time and rise time, β is set below 0.7. In our simulation, we opted for β to be 0.9 as our goal was to specifically reduce overshoot. Additionally, we employed a population size of 20 and 10 generations. The applied GA algorithm found the following value to be the best for the controller: $K_p = 8.985 \times 10^{-3}$, $K_i = 8.985$, $K_d = 8.046 \times 10^{-5}$ and $\tau = 7.551 \times 10^{-5}$.

3 Simulation and results of FSM control with an ideal sensor

This section presents simulation results for both the GA-optimized PID controller and the SISO-tuned controller.

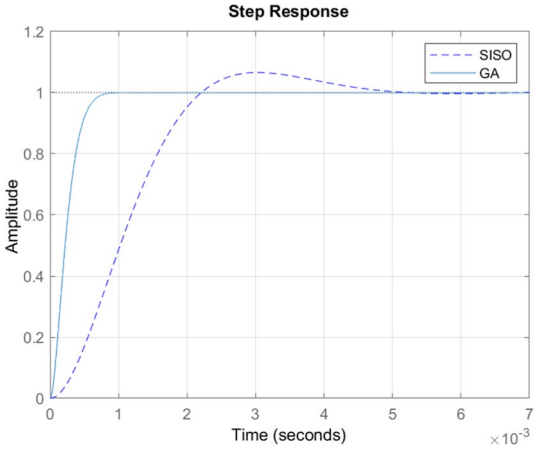

Fig. 4 Illustrates the closed feedback control loop response of the FSM to step input when employing the SISO tuned as well as the GA tuned controller

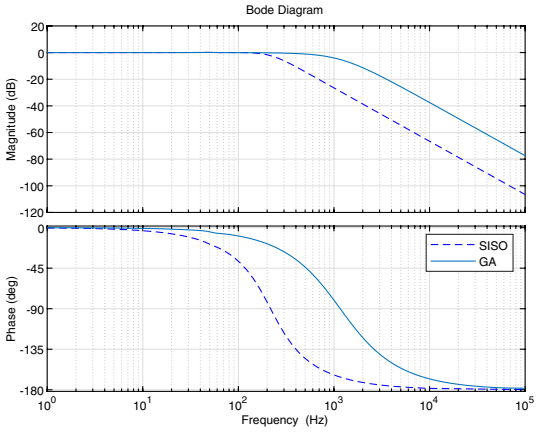

Fig. 5 Bode plot comparison of the two controllers

Performance comparisons between the two controllers are based on parameters such as overshoot, rise time, settling time, and steady-state error. Figures 4 and 5 respectively display the closed-loop step response and the Bode plot for the two controllers. The GA-optimized PID controller achieves no overshoot and exhibits faster rise time and quicker settling behavior compared to the SISO-tuned controller. Additionally, it achieves increased closed-loop bandwidth, making it well-suited for the swift responses required in beam steering applications for FSO communication.

The faster rise time and quicker settling behavior compared to the SISO tuned PID controller shows that with the GA fine tuned controller, the system reaches its steady state more quickly. This means it can rapidly respond to changes, a crucial requirement in the beam steering system. The increased closed-loop bandwidth indicates that it has a wider range of frequencies over which the system can effectively track changes in the desired output. In practical terms, the system can accurately track or reject faster changing inputs. The results for the simulations of the two controller types are presented in Table 2. From this point on wards, the PID gains used are those obtained using the GA optimization.

Table 2 Comparison of the two controllers

Property	PID−Ga	PID−SISO
Overshoot	0	0.06574
Rise time (sec)	4.0129×10^{-4}	0.00146
Settling time(sec)	6.6313×10^{-4}	4.37×10^{-3}
Steady state error	4.077×10^{-4}	1.47×10^{-3}
Closed loop bandwidth	853 Hz	234 Hz

4 Proposed model for position sensing

During the process of tuning the PID gains, an ideal sensor was initially assumed to exist within the sensor path. However, in a practical scenario, a real sensor is installed to provide position information regarding the incident laser spot. As previously stated, this work leverages QD for beam spot position detection task.

The QD is a device with light-sensitive surface, used in tracking, alignment, and position determination systems. It consists of four identical P-N junction photodiodes, referred to as quadrants, separated by a thin inactive region, as shown in Fig. 6. When the incident light interacts with the QD, it triggers each of the photodiodes to generate electric signals. These signals are used in determining the position of the incident laser spot on the surface of QD. However, the nonlinearities of the QD negatively impact the accuracy of laser spot position detection. To address this problem, our previous work developed a stacking neural network ensemble model designed to enhance the accuracy of laser spot position determination on the QD. The ensemble combined multiple artificial neural network (ANN) models, specifically five Radial Basis Function Neural Networks (RBFNNs) as base learners and a Feedforward Neural Network (FFNN) as a meta-learner. Simulation results demonstrated that our ensemble solution significantly improved detection accuracy, making it a viable choice for precise position detection in laser communication systems. More details can be found in Baleya et al. (2023). This model has also been used in our current work.

There are two approaches to develop and deduce the QD model. The first approach involves using theory-based first principles. In this approach, one might consider the

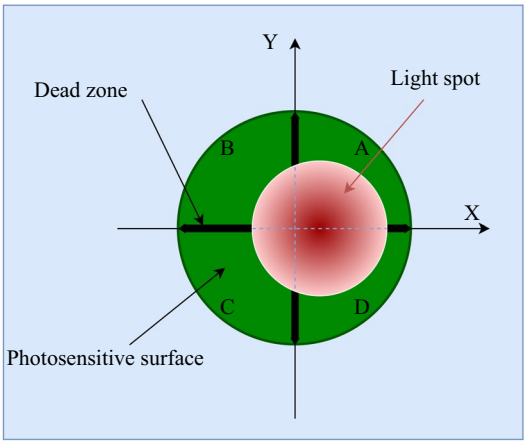

Fig. 6 An illustration of the photodiodes' configuration on the detector and highlighting the incidence of a light spot

QD's geometry, beam power, beam size, and model the conversion from optical power to electric signals. By understanding the displacement of the beam spot from the center of the detector, one can determine the portion of the beam that irradiates each photodiode and obtain the electrical signal output from each photodiode. The second approach is data-driven, it relies on collecting data from the actual QD, comprising of the spot positions and corresponding photoelectric signals. Using this data, a model is fit that maps the relationship between spot position and the QD output electric signals can be fitted.

This work employs the later approach. The choice is driven by the availability of QD experimental data from obtained from Li et al. (2019), which provides valuable insights into the QD's behavior. The data was obtained from the QD with a radius of 1.5 mm. Observations were made on the QD along the x-axis, between -0.5 mm and 0.5 mm. 501 data samples collected using 0.75 mm incident beam radius are used for modeling the QD dynamics. A single hidden layer FFNN is used for this purpose. The input to the network is the x position and the network outputs the corresponding voltages. Finding the number of neurons in the hidden layer that give best model performance becomes the main task. In determining the optimal value for the number of the neurons in the hidden layer, the neurons are varied from 1 to 20, for each neuron number, a neural network is trained 100 times and each time the data is randomly split into 80 % training and 20 % validation sets, then the training and validation RMSE are recorded. Different split result in different RMSE values which are then averaged. The averaged RMSE values are more accurate and more statistically significant allowing us to pick more confidently the best number of neurons to be employed in the hidden layer of the model. Figure 7 shows the trend in the training and variation errors during this process. As depicted in the figure, the FFNN with 10 neurons resulted in best performance on the validation set. It is important to note that the network is trained using the Levenberg-Marquardt algorithm and the neurons in the hidded layer are activated using the hyperbolic tangent sigmoid function, while the output neaurons are activated by pureline transfer function. Finally, the FFNN with 10 neurons in the hidden layer was trained to capture the QD behavior.

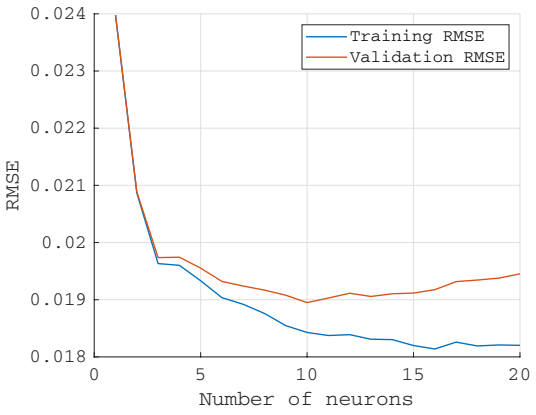

Fig. 7 An illustration of the training and validation errors as the hidden layer's neuron count rises from 1 to 20 during QD modeling

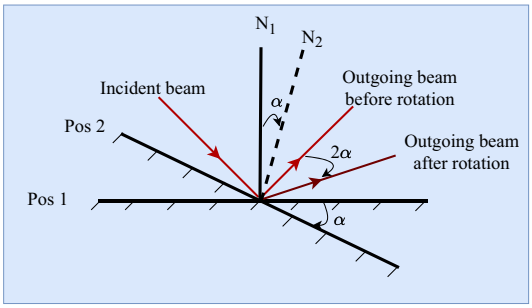

Fig. 8 Depicts the relationship between the rotating mirror's angular displacement and the resulting optical angle displacement in the outgoing beam

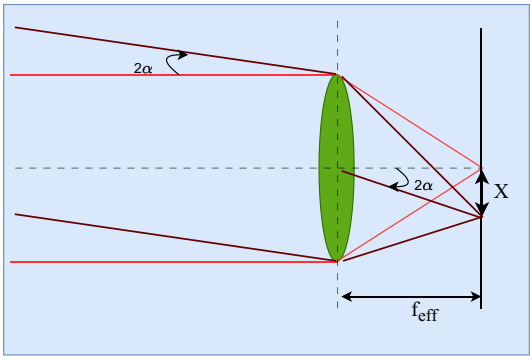

Fig. 9 Optical angular displacement to lateral displacement on the detector surface

5 Integration of QD in the closed feedback control loop for the FSM

Fig. 1 provides a visual representation of the impact of FSM actuation on the laser beam. A detailed illustration of the mirror's operation on the laser beam is shown in Fig. 8. Initially, the mirror is at position (Pos 1). When the mirror is rotated from its initial position (Pos 1) to position (Pos 2) with an angular displacement of α, a corresponding angular change of 2α is induced in the outgoing beam.

After establishing the relationship between the mirror's angular displacement and the resulting optical displacement, it becomes crucial to examine the impact of this optical shift on the detector. Specifically, the angular shift in the optical beam manifests as a lateral displacement on the QD surface. This situation is illustrated in Fig. 9, as described in Grigorov (2008).

This interplay between angular and lateral displacements is crucial for understanding the behavior of the beam steering system employing QD and FSM. The relationship between the optical angle and the lateral displacement is mathematically given by:

$$x = \mathrm{f}_{eff} \tan(2\alpha), \tag{6}$$

where x is the lateral displacement on the detector, f_{eff} denotes the effective focal length between the converging lens and the QD and 2α is the change in the optical angle. The modeled sensor and the laser spot position approximator are connected in the sensor path and system behavior is simulated in Simulink. The final arrangement is depicted in Fig. 10.

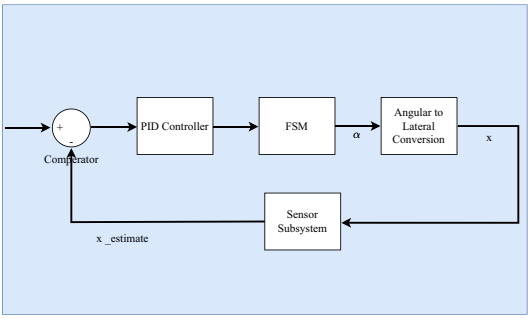

Fig. 10 The final setup for the FSM closed feedback control loop

6 Simulation and results of FSM control with a QD sensor

Table 3 summarizes the simulation results for the proposed GA tuned PID controller when applied to the FSM system with the two different types of sensors: an ideal sensor and the QD sensor. The results reveal that the use of the QD sensor leads to an increase in the overshoot. The overshoot goes from 0 to 0.0737, compared to the ideal sensor. This increase could potentially be attributed to the detection errors induced by the actual QD sensor. It is important to note that while this is a slight increase, it could have significant implications, however, it is normally corrected manually during system installation.

Interestingly, while there is an increase in overshoot with the QD sensor in place, good responses are observed. This indicates that the system can quickly adjust to changes, maintaining the line-of-sight (LOS) more effectively. The faster settling time results in lower latency in communication, enhancing real-time data transmission. Additionally, quicker stabilization of the beam reduces the chances of misalignment due to disturbances. Finally, precise and rapid adjustments improve the overall accuracy of the beam steering system, which is crucial for high-data-rate communication.

These results suggest that our GA-optimized controller achieves good performance for the beam steering system. However, it is important to consider the trade-off between overshoot and settling time. Depending on the specific requirements of the system, one may prioritize minimizing overshoot or reducing settling time. Therefore, the choice of sensor should be made carefully, taking these trade-offs and the specific needs of the application into account.

Table 3 A comparison of the system's step response with QD sensor to its response with ideal sensor

Property	Ideal Sensor	QD Sensor
Overshoot	0	0.07
Rise time	4.01×10^{-4} sec	2.11×10^{-4} sec
Settling time	6.63×10^{-4} sec	6.11×10^{-4} sec
Steady state error	4.08×10^{-4}	1.39×10^{-4}

7 Conclusion

This work assesses the combined functionalities of sensor, controller, and actuator in achieving precise beam steering functionality in FSO communication. This has been accomplished by firstly using GA to optimize the PID controller within the FSM closed loop, which demonstrates improved time response characteristics as well no overshoot compared to the SISO tuned controller. Next, a QD sensor has modeled and integrated it into the system. Simulations reveal that while the QD sensor slightly increases overshoot, a faster and more responsive FSM closed feedback control loop is attainable. These findings translate to benefits for the beam steering system in FSO communication. As such this work establishes a valuable framework for optimizing optical beam steering systems in FSO communication. By understanding the trade-offs between sensor characteristics, actuator characteristics and system performance, future research can explore advanced sensor and actuator technologies to achieve even tighter beam steering control while minimizing latency and overshoot in the actuation device. As such, this work paves way for the development of next-generation FSO systems with superior performances.

Acknowledgements The authors gratefully acknowledge the support received from the Mission Department of Egypt's Ministry of Higher Education, the Egypt-Japan University of Science and Technology (E-JUST), and the TICAD 7 African Scholarship for this work.

Funding The authors have not disclosed any funding.

Data availability Data used in this study will be made available upon request.

Declarations

Conflict of interest The authors affirm that there are no existing financial conflicts or personal associations that might seem to affect the findings presented in this paper.

References

Chaudhry, A.U., Yanikomeroglu, H.: Free space optics for next-generation satellite networks. IEEE Consum. Electron. Mag. **10**, 21–31 (2020)

Al-Gailani, S.A., et al.: A survey of free space optics (FSO) communication systems, links, and networks. IEEE Access **9**, 7353–7373 (2020)

Watkins, R.J., Chen, H.-J., Agrawal, B.N., Shin, Y.S.: Optical beam jitter control. Free-Space Laser Commun. Technol. XVI **5338**, 204–213 (2004)

Zhou, Q., Ben-Tzvi, P., Fan, D.: Design and analysis of a fast steering mirror for precision laser beams steering. Sens. & Transducers **5**, 104–118 (2009)

Chaudhary, H., Khatoon, S., Singh, R., Pandey, A.: Modeling and simulation of fast steering mirror plant for laser beam pointing application (2018)

Zhang, S., et al.: A method of enhancing fast steering mirror's ability of anti-disturbance based on adaptive robust control. Math. Problems Eng. **1**, 1-9 (2019)

Zhu, W., Bian, L., An, Y., Chen, G., Rui, X.: Modeling and control of a two-axis fast steering mirror with piezoelectric stack actuators for laser beam tracking. Smart Mater. Struct. **24**, 075014 (2015)

Zhang, J., et al.: Advances in InGaAs/InP single-photon detector systems for quantum communication. Light & Sci. Appl. **4**, e286–e286 (2015)

Wang, X., et al.: A method for improving the detection accuracy of the spot position of the four-quadrant detector in a free space optical communication system. Sensors **20**, p.7164 (2020)

Zhang, C., et al.: Research of intelligent segment-fitting algorithm for increasing the measurement accuracy of quadrant detector in straightness measuring system. Opt. & Laser Technol. **125**, 106062-106070 (2020)
Silva, E., Van Vliet, K.: Robust approach to maximize the range and accuracy of force application in atomic force microscopes with nonlinear position-sensitive detectors. Nanotechnology **17**, 5525-5530 (2006)
Li, Q., et al.: A new response approximation model of the quadrant detector using the optimized BP neural network. IEEE Sens. J. **20**, 4345–4352 (2019)
Qiu, Z., et al.: Neural-network-based method for improving measurement accuracy of four-quadrant detectors. Appl. Optics **61**, F9–F14 (2022)
Lu, C., et al.: A novel method to improve detecting sensitivity of quadrant detector. Optik **125**, 3519–3523 (2014)
Wang, X., et al.: Method to improve the detection accuracy of quadrant detector based on neural network. IEEE Photonics Technol. Lett. **33**, 1254–1257 (2021)
Wu, J., Chen, E.: A novel nonparametric regression ensemble for rainfall forecasting using particle swarm optimization technique coupled with artificial neural network (2009)
Baleya, M., Shalaby, H., Kato, K., Elsabrouty, M.: Neural network ensemble for precise laser spot position determination on a quadrant detector. IEEE Photonics Technol. Lett. **36**, 115–118 (2023)
Man, K.-F., Tang, K.-S., Kwong, S.: Genetic algorithms: concepts and applications [in engineering design]. IEEE Trans. Industr. Electron. **43**, 519–534 (1996)
Deniz, F.N., Yüce, A., Tan, N., Atherton, D.P.: Tuning of fractional order pid controllers based on integral performance criteria using fourier series method. IFAC-PapersOnLine **50**, 8561–8566 (2017)
Jayachitra, A., Vinodha, R.: Genetic algorithm based pid controller tuning approach for continuous stirred tank reactor. Adv. Artif. Intell. **2014**, 9–9 (2015)
Gaing, Z.-L.: A particle swarm optimization approach for optimum design of pid controller in avr system. IEEE Trans. Energy Convers. **19**, 384–391 (2004)
Grigorov, C.: Evaluation of coarse- and fine-pointing methods for optical free space communication (2008). https://urn.kb.se/resolve?urn=urn:nbn:se:ltu:diva-45230. Dissertation